

# EFFECTS OF NANO-Fe<sub>3</sub>O<sub>4</sub> AND HYDROGEN SULFIDE ON ALLEVIATING HEAVY METAL TOXICITY IN CUCUMBER SEEDLING

QIAO, L.\* – LIU, H. – HU, C. – HU, L. – DU, H.

*College of Life Science and Agronomy, Zhoukou Normal University, Zhoukou 466001, China*

*\*Corresponding author  
e-mail: qiaolin2012@126.com*

(Received 15<sup>th</sup> Sep 2018; accepted 12<sup>th</sup> Nov 2018)

**Abstract.** The possible role of reducing effects of nano-Fe<sub>3</sub>O<sub>4</sub> and hydrogen sulfide on alleviating heavy metal toxicity in germinating cucumber seedling was investigated. The toxic effects of Fe<sub>3</sub>O<sub>4</sub> nanoparticles (NPs) (6, 50, 100 nm), and bulk were evaluated in cucumber plants. Among the synthesized nano-Fe<sub>3</sub>O<sub>4</sub>, only the small size (6 nm) had significant inhibit effect on fresh and dry biomass of cucumber seedlings. cucumber seedlings grown under lowest concentrations of 50 mg/L nano-Fe<sub>3</sub>O<sub>4</sub> (6 nm) were affected by a decrease in biomass and enzyme activities compared to control. However, at higher concentration of nano-Fe<sub>3</sub>O<sub>4</sub> dosage (2000 mg/L), there was significant increase in biomass and enzymatic activities of superoxide dismutase (SOD) and peroxidase (POD), respectively. The toxicity effects of the different sizes of nano-Fe<sub>3</sub>O<sub>4</sub> particles and bulk-Fe<sub>3</sub>O<sub>4</sub> might depend on the chemical composition, the structure properties/ particle sizes, the concentration in the tested medium, the time of incubation, as well as the plant species.

**Keywords:** *heavy metal toxicity, toxic mechanism, magneto dipole interaction, nano-Fe<sub>3</sub>O<sub>4</sub>, cucumber seedling*

## Introduction

Due to the anticipated high-volume production and widespread use in coming years, engineered nano-materials will inevitably be released into the environment and interact with plants during manufacture, use, and disposal. Magnetic (Fe<sub>3</sub>O<sub>4</sub>) nanoparticles have been widely investigated for their scientific interests but also their technological application in many fields (ferrofluids, biomedicines, magnetic records, catalysts and electronic technique) due to their biological compatibility and magnetic properties (Shen et al., 2013). Iron oxide nanoparticles are among the primary nano-materials used in biomedical fields due to their magnetic property and high chemical stability (Xiao et al., 2011). Co-precipitation method and high-temperature decomposition are the two methods commonly used to prepare iron oxide nanoparticles. However, reactions of co-precipitation do not furnish excellent control of size distribution and crystallinity of the resulting particles; they are also thermodynamically driven (Laurent et al., 2008; Vinod et al., 2012; Jain et al., 2008). On the other hand, the use of FeOx NPs produced with high-temperature decomposition reactions of metal-organic compounds is limited because they are soluble only in organic solvents. The preparation of water-dispersible iron oxide nanoparticles with suitable surface coatings provides a major challenge in nanotechnology. In the present study, we synthesized water-soluble small iron oxide nanoparticles by the chemical reduction method using vitamin C as the reducing agent by oxidizing its C=C double bond. It has been reported that the magnetic property of magnetic (Fe<sub>3</sub>O<sub>4</sub>) nanoparticles could depend on their particle sizes (Roca et al., 2007). The polyol-mediated method is a versatile chemical system to prepare excellent-quality

water-stable Fe<sub>3</sub>O<sub>4</sub> nanoparticles (Shen et al., 2013). In this synthesis approach, polyols (ethylene glycol (EG), diethylene glycol (DEG), triethylene glycol or poly-ethylene glycol) are usually used as solvent and reductant and play a stabilizer role to control the growth of particles and prevent inter-particle aggregation (Liu et al., 2009; Miguel-Sancho et al., 2011). Magnetic (Fe<sub>3</sub>O<sub>4</sub>) nanoparticles synthesized with this method can exhibit some water dispersibility, compared to the thermal decomposition method. This might be dependent on the hydrophilic coating (Liu et al., 2009). In the present work, the polyol-mediated method was used as the second method to prepare magnetic (Fe<sub>3</sub>O<sub>4</sub>) nanoparticles: 50 nm and 100 nm, using ethylene glycol (EG) as the solvent and reductant. The TEM images, XRD, vibrating sample magnetometer (VSM), Fourier transform infrared (FTIR) spectroscopy and thereto gravimetric analyses (TGA) were used in this study to characterize the synthesized nanoparticles and bulk. The aim of this paper is to research on the effects of nano-Fe<sub>3</sub>O<sub>4</sub> and hydrogen sulfide on alleviating heavy metal toxicity in germinating cucumber seedling.

## Materials and Methods

Photosynthesis of cucumber can be best accumulated at 25~32 °C. During the morning, the temperature should be maintained at around 25 °C, and the temperature will be slightly reduced in the afternoon. Carbon dioxide fertilized in the morning. In order to promote nutrient transport and reduce plant consumption, the temperature should be controlled in the first half of the night at 16-18 °C and in the second half of the night at 10-14 °C. The optimum temperature for root growth is 20~23 °C, the lowest temperature is 8~12 °C, and the highest temperature is 32~38 °C. The temperature of root growth is no less than 15 °C.

## Chemicals

Different chemicals were used to synthesize different sizes of magnetic (Fe<sub>3</sub>O<sub>4</sub>) nanoparticles. In general, ferric chloride hexahydrate (FeCl<sub>3</sub>·6H<sub>2</sub>O), sodium hydrogen carbonate (NaHCO<sub>3</sub>), ascorbic acid or vitamin C (C<sub>6</sub>H<sub>8</sub>O<sub>6</sub>), ethylene glycol C<sub>2</sub>H<sub>6</sub>O<sub>2</sub>, 1,6-Hexanediamine (C<sub>6</sub>H<sub>16</sub>N<sub>2</sub>), and sodium acetate (CH<sub>3</sub>COONa), also abbreviated NaOAc were used as shown in the *Table 1* to synthesize nanoparticles of 6, 50 and 100 nm sizes.

**Table 1.** Chemicals used to synthesis nano-Fe<sub>3</sub>O<sub>4</sub> (6 nm, 50 nm, and 100 nm)

N	Chemical composition				Autoclave		
					Temperature (°C)	Time (min)	Size (nm)
I	FeCl <sub>3</sub> ·6H <sub>2</sub> O(0.54g)	NaHCO <sub>3</sub> (1.52g)	VC(0.06g)	H <sub>2</sub> O(35ml)	150	240	6
II		NaOAc(2g)	1,6-Hexa(6.7ml)		198		50
	FeCl <sub>3</sub> ·6H <sub>2</sub> O(1g)			EG(30ml)		360	
III		NaOAc(1g)	1,6-Hexa(7ml)		205		100

The mini-Q quality water was used for all reactions and preparation procedures. All glassware used in the synthesis processes of magnetic (Fe<sub>3</sub>O<sub>4</sub>) nanoparticles were

thoroughly cleaned several times in aqua regia (HCl: 3 parts and HNO<sub>3</sub>: 1 part); then rinsed with water mini-Q and dried at 60 °C before being used (Burman et al., 2004; Garg et al., 2006).

### **The Magnetic (Fe<sub>3</sub>O<sub>4</sub>) Nanoparticles**

Magnetic (Fe<sub>3</sub>O<sub>4</sub>) nanoparticles (6 nm) were synthesized following the procedure from Xiao et al. (2011), with some modification (*Figure 1*). In a typical Fe<sub>3</sub>O<sub>4</sub> nanoparticles, a 15 mL of 0.54 g (FeCl<sub>3</sub> · 6H<sub>2</sub>O) aqueous solution was first vigorously mixed with 20 mL of 1.52 g NaHCO<sub>3</sub> aqueous solution, then the mixture solution was stirred for 30 min to form a yellow solution. About 0.06 g of vitamin C was added into the first solution and the mixture stirred for 10 min before being transferred into an autoclave that was kept at 150 °C for 4h. After being allowed to cool at a room temperature, the black products were collected by magnetic separation and washed three times with water (Millipore, resistivity > 18.2 MΩ · cm<sup>-1</sup>) and ethanol. The residue obtained was dried at 60 °C before being analyzed and used.

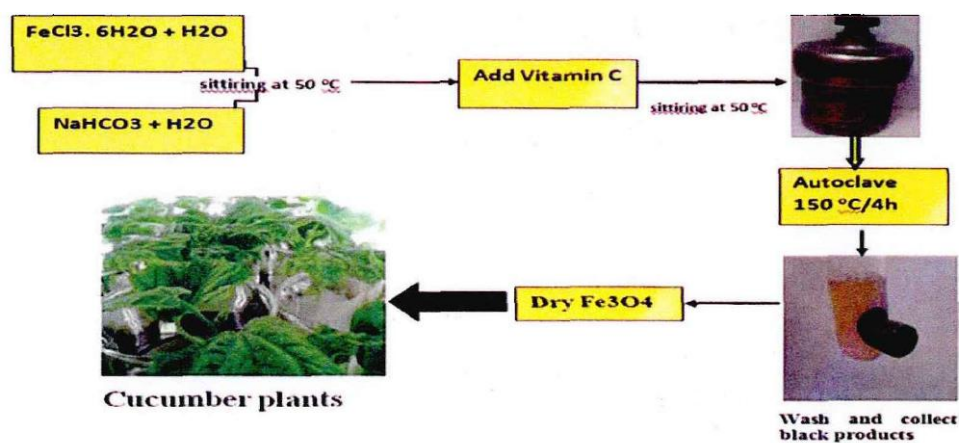


**Figure 1.** Synthesis procedures of magnetic (Fe<sub>3</sub>O<sub>4</sub>) nanoparticles (6 nm)

Magnetic (Fe<sub>3</sub>O<sub>4</sub>) nanoparticles (50 nm and 100 nm) were synthesized following some modification of the procedures from Yin et al. (2013). For Fe<sub>3</sub>O<sub>4</sub> (50 nm), 1 g (FeCl<sub>3</sub> · 6H<sub>2</sub>O) and 2 g (NOAc) were first vigorously mixed with 30 mL of EG (Ethylene glycol). Then 6.5 mL of 1,6-hexanediamine was added into the first solution and the mixture stirred for another 10 min before being transferred into an autoclave that was kept at 198 °C for 6 h. The synthesis procedure of 50 nm and 100 nm were similar. The only difference was in the addition of 1 g NOAc), 7 mL of 1,6-hexanediamine and boiled at 205 °C for 6 h in the synthesis of nano-Fe<sub>3</sub>O<sub>4</sub> (100 nm). All procedures after autoclaving were similar to those of Fe<sub>3</sub>O<sub>4</sub> (6 nm).

The morphology, particle shape and structure of Fe<sub>3</sub>O<sub>4</sub> NPs were determined by Scanning Electron Microscopy (SEM, S-4800, HITACHI, Japan) and Transmission Electron Microscope TEM (JEM 200CX, Japan), respectively. For TEM analysis, the Fe<sub>3</sub>O<sub>4</sub> NPs or bulk-Fe<sub>3</sub>O<sub>4</sub> were dispersed in deionized water and sonicated for 40 min. Then, some suspension liquid was dropped on a copper grid for Transmission Electron Microscopy (TEM) observation (Zhang et al., 2011). The TEM pictures were obtained from Tecnai G2 20 S-Twin transmission electron microscope 119 (FEI company, Japan)

operating at 200 kV. The mean size, size distribution, and Zeta potential of 50 mg/L magnetic (Fe<sub>3</sub>O<sub>4</sub>) nanoparticles or bulk-Fe<sub>3</sub>O<sub>4</sub> were measured by Dynamic Light Scattering (DLS) equipment (ZETA SIZER 90, Nano series, Malvern, UK) in deionized water and nutrient solution (pH 5.5). FT-IR spectra were obtained using Fourier transform infrared spectroscopy (FTIR Tensor 27, Broker, Germany) analysis. The magnetic property was determined using the vibrating sample magnetometer (VSM, 7410, Lake Shore, USA). The crystal structure of the synthesized nanoparticles or bulk was obtained by X-ray diffraction, XRD (XRD, X'pert PRO MPD, Holland) measurement. To collect 20 data from about 10 °C to 90 °C, we used a continuous scanning mode. Thermo gravimetric analysis (TGA) was carried out for powder samples using a NETZSCH STA 449C thermo gravimetric analyzer.

To combat against adverse environmental heavy metal toxicity, plants have developed potential mechanisms such as enzymatic activities (SOD and POD) and the production of low molecular weight thiols. Naturally, plants show differences in their capacity of heavy metals tolerance. Some plants can grow in metal-contaminated soils with high level, while other groups could not grow even at low concentration. The fresh roots or shoots (0.2 g) from each treatment were homogenized with 1.8 mL of 0.05M sodium phosphate buffer (PH 7.8) under ice bath to make 10% sample compound liquid. The homogenate was centrifuged at 10.000 mg and 4 °C for 15 min. Then, the supernatant was used for superoxide dismutase (SOD) and MDA contents. The SOD activity was analyzed by determining the ability to inhibit the photochemical reduction of nitroblue tetrazolium at 550 nm.

## Results

Figure 2 shows the XRD patterns of the synthesized magnetic (Fe<sub>3</sub>O<sub>4</sub>) nanoparticles with different sizes and bulk-Fe<sub>3</sub>O<sub>4</sub>.

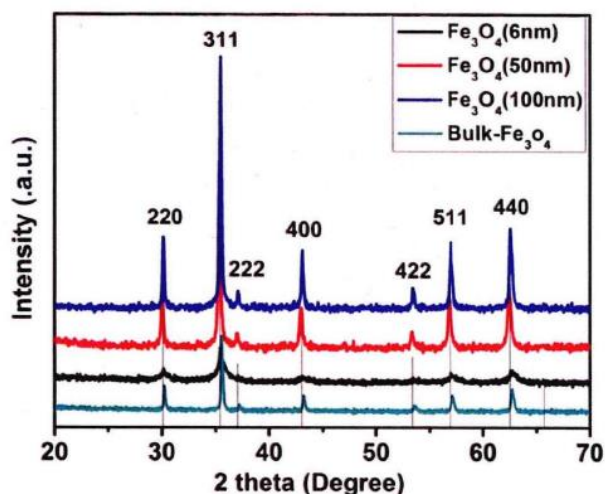
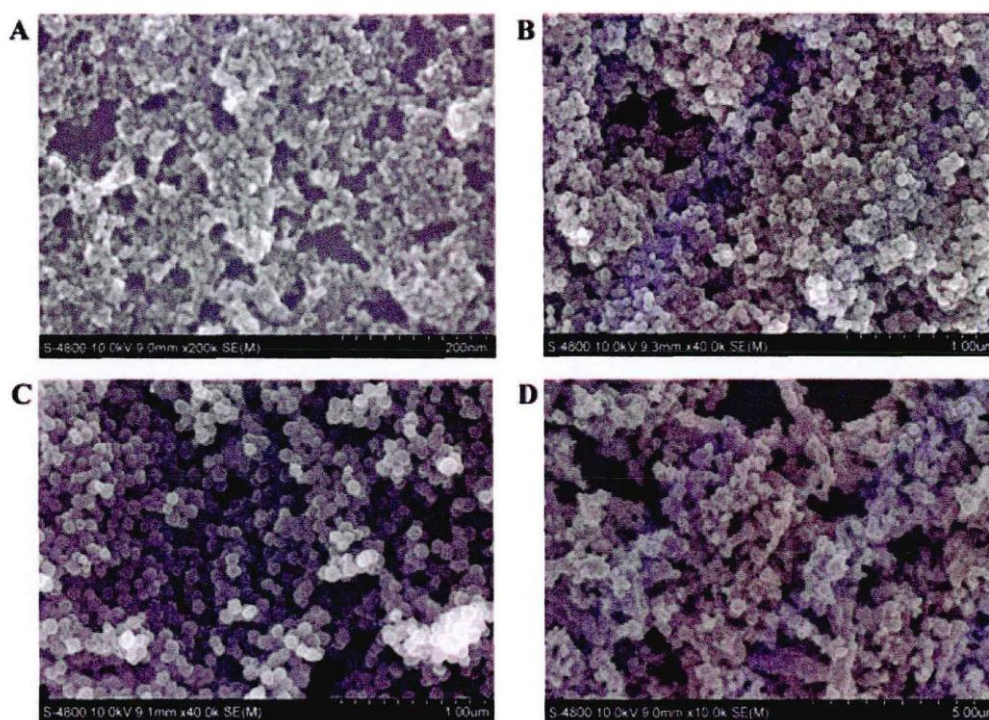


Figure 2. XRD patterns of Fe<sub>3</sub>O<sub>4</sub> nanoparticles (6 nm, 50 nm, and 100 nm), and Bulk-Fe<sub>3</sub>O<sub>4</sub>

In this study, the characteristic peaks observed in the XRD pattern at 2θ of 30.09, 35.42, 37.05, 43.05, 53.39, 56.94, 62.51 were corresponding to the diffractions of 220, 311, 222, 400, 422, 511 and 440 lattice planes of inverse cubic spinet structure of Fe<sub>3</sub>O<sub>4</sub>

NPs and Fe<sub>3</sub>O<sub>4</sub>-Bulk. As shown in *Figure 2*, all XRD patterns had a diffraction peak at  $2\theta=35.42^\circ$  corresponding to the spinel phase of the synthesized (Fe<sub>3</sub>O<sub>4</sub>) nanoparticles or bulk. The decrease in the intensity after the diffraction peaks at  $2\theta=35.42^\circ$  could be attributed to the formulation of more crystalline phase particles in all annealed magnetic (Fe<sub>3</sub>O<sub>4</sub>) nanoparticles and the bulk-Fe<sub>3</sub>O<sub>4</sub>. The results show that the spinel structures are in good agreement with the XRD standard for the magnetic nanoparticles and no peaks of impurities were observed in the XRD pattern, indicating that the synthesized particles powders are magnetic (Fe<sub>3</sub>O<sub>4</sub>) nano-particles.

The properties of nanomaterial strongly depend upon the dimension of nanoparticles. Hence, the control of particle size is very important in nanotechnology study or nanoparticles application. In order to analyze the morphology and particles size of the synthesized magnetic (Fe<sub>3</sub>O<sub>4</sub>) nanoparticles and bulk-Fe<sub>3</sub>O<sub>4</sub>, SEM images of particles were taken. The results are presented in the *Figure 3*.



**Figure 3.** SEM images of Fe<sub>3</sub>O<sub>4</sub> nanoparticles 6 nm (A), 50 nm (B), 100 nm (C) and bulk-Fe<sub>3</sub>O<sub>4</sub>(D)

The SEM images showed that spherical magnetic (Fe<sub>3</sub>O<sub>4</sub>) nanoparticles (*Figure 3A,B and C*) were obtained from all methods of synthesis used in this study. The SEM images of the synthesized Fe<sub>3</sub>O<sub>4</sub> nanoparticles (*Figure 3A*) showed that the materials obtained were made of small particles. As showed in *Figure 3*, Fe<sub>3</sub>O<sub>4</sub> nanoparticles (small size) are found to be interconnected with least agglomeration which might be due to their high surface charge and the magneto dipole interaction.

## Discussion

The *Figure 4* shows representative TEM images of the synthesized magnetic (Fe<sub>3</sub>O<sub>4</sub>) nanoparticles with diameters of  $6.82\pm 1.38$  nm;  $52.56\pm 8.01$  nm;  $100.66\pm 15.62$  nm,

respectively. We observed that the sizes of all synthesized nanoparticles were smaller compared to bulk-Fe<sub>3</sub>O<sub>4</sub> (144.27±28.95 nm). The size histograms of the synthesized nanoparticles and bulk based on statistical analysis of over 90 particles are shown in the *Figure 4a-d*. The measurement of the particle diameters of all synthesized magnetic (Fe<sub>3</sub>O<sub>4</sub>) nanoparticles showed a normal distribution curve after ultra-sonication dispersal as compared to bulk (*Figure 4a-d*). Similar observation has been reported by Shen in 2013 (Shen et al., 2013), who synthesized and characterized water-soluble ultra-small Fe<sub>3</sub>O<sub>4</sub> nanoparticles for potential bio-application.

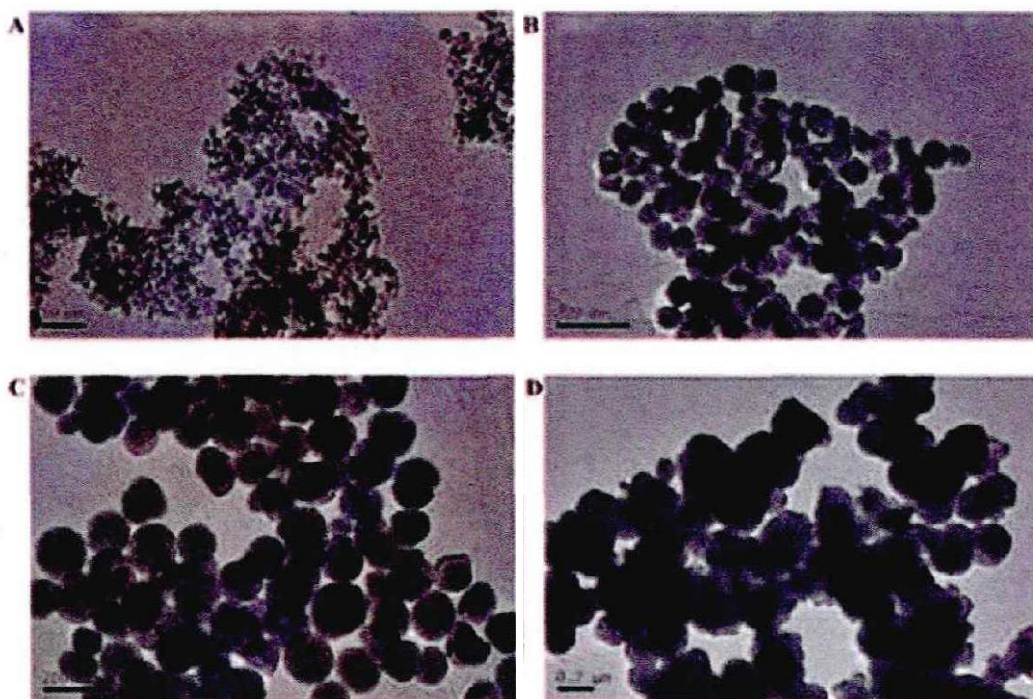


**Figure 4.** TEM images and size distribution histogram of Fe<sub>3</sub>O<sub>4</sub> NPs: 6 nm (A-a), 50 nm (B-b), 100 nm (C-c) and Bulk-Fe<sub>3</sub>O<sub>4</sub>, (D-d)

When suspended in water or nutrient solution, the hydrodynamic diameters of the 50 mg/L of all sizes of the synthesized nanoparticles and bulk-Fe<sub>3</sub>O<sub>4</sub> were larger than the results measured by their corresponding TEM images. This is due to their agglomeration. The *Table 2* shows that nano-Fe<sub>3</sub>O<sub>4</sub> particles were largely aggregated.

**Table 2.** Size distribution and zeta potentials of nano- and bulk- Fe<sub>3</sub>O<sub>4</sub>

Nanoparticles or bulk	Water		Nutrient solution	
	<DH>nm	ξ-potential (mV)	<DH>nm	ξ-potential (mV)
Fe <sub>3</sub> O <sub>4</sub> (6nm)	255±9.1	-12.66±0.4	433.3±42.2	-15.9±0.2
Fe <sub>3</sub> O <sub>4</sub> (10nm)	242.2±0.6	27.9±0.4	741.1±39.6	-16.6±1.3
Fe <sub>3</sub> O <sub>4</sub> (100nm)	184.7±4.1	29±0.1	911.5±35.3	-13.5±1.1
bulk- Fe <sub>3</sub> O <sub>4</sub>	1041±150.8	9.8±0.6	1402±118.9	-18.8±0.1

In water, the aggregation level appeared in the order of 6 nm > 50 nm > 100 nm with the particles averaging 255±9.1 nm, 242.2±6.6 nm and 184.7±4.1 nm, respectively. The practical averages in nutrient solution were 433±42.2 nm, 741±39.6 nm, 911±35.3 nm, and 1402±118.9 nm respectively for 6 nm, 50 nm, and 100 nm. The change in the order of the aggregation level (100 nm > 50 nm > 6 nm) in the nutrient solution could be due to the presence of additional chemicals in the nutrient solution. We observed that the hydrodynamic diameters of all nanoparticles were smaller in water and nutrient solution compared to bulk-Fe<sub>3</sub>O<sub>4</sub>, (1041±150.8 nm in water and 1402±118.9 nm in nutrient solution).

The modification of the synthesized magnetic (Fe<sub>3</sub>O<sub>4</sub>) nanoparticles with different sizes (6 nm, 50 nm, and 100 nm) and bulk-Fe<sub>3</sub>O<sub>4</sub> surfaces for their stabilization were analyzed and confirmed by Fourier Transform Infrared Spectroscopy (FTIR) as shown in the *Figure 5*.

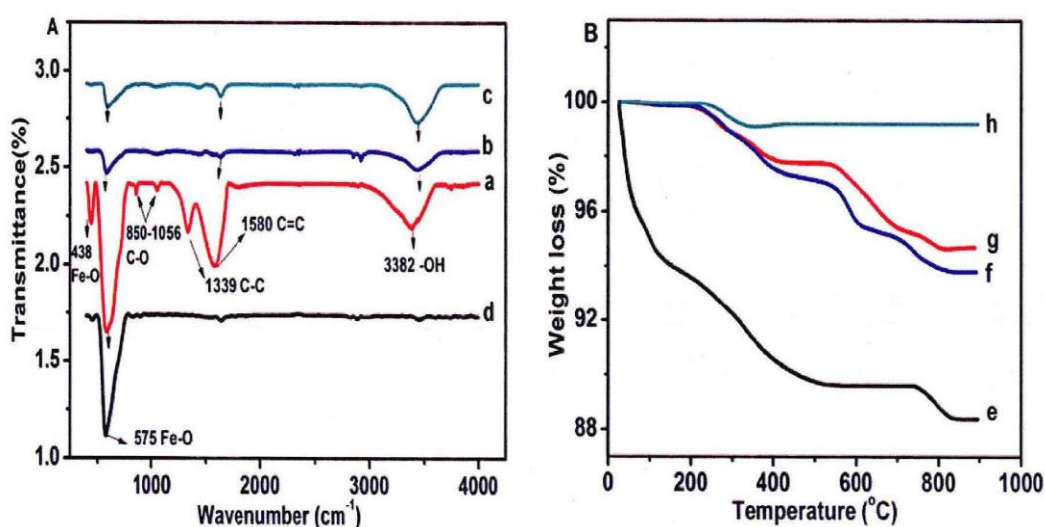


**Figure 5.** FTIR Analysis of Fe<sub>3</sub>O<sub>4</sub> nanoparticles (Aa-c) and Bulk- Fe<sub>3</sub>O<sub>4</sub>, (Ad), TGA curves of Fe<sub>3</sub>O<sub>4</sub> nanoparticles (Be-f) of bulk- Fe<sub>3</sub>O<sub>4</sub> (Bh)

In general, the stretching absorption peaks of Fe-O at 575 cm<sup>-1</sup> appeared in the FTIR spectra of all the synthesized nanoparticles and bulk (*Figure 2-SAa-d*). In addition, the peaks in the region numbers 438-575 cm<sup>-1</sup> are also attributed to the Fe-O vibration (*Figure 5*). In the FTIR spectra of the nano-Fe<sub>3</sub>O<sub>4</sub> (6 nm), the peaks around 850-1056 cm<sup>-1</sup>, 1342 cm<sup>-1</sup> and 1580 cm<sup>-1</sup> were related to the group C-O, C-C and C=C respectively (*Figure 5*). The double bonds of C=C were due to the additional compounds, mainly the Vitamin C in using chemicals for the synthesis of nano-Fe<sub>3</sub>O<sub>4</sub> (6 nm). The peak observed in the region number 3382 cm<sup>-1</sup> was related to the vibration of -OH. This peak (around 3382 cm<sup>-1</sup>) was found in the FTIR spectra of all synthesized nanoparticles (6 nm, 50 nm, and 100 nm). However, it was not observed in the bulk spectra (*Figure 5*). The FTIR spectra analysis suggests that the characteristic stretching absorption peaks at 575 cm<sup>-1</sup> corresponding to the Fe-O was related to the magnetite phase. *Figure 5 (Be-h)* shows the weight loss curves of magnetic (Fe<sub>3</sub>O<sub>4</sub>) nanoparticles (6 nm, 50 nm, and 100 nm) and bulk-Fe<sub>3</sub>O<sub>4</sub> at different stages of surface modification. It appeared that below 200 °C, the weight loss was insignificant for nano-Fe<sub>3</sub>O<sub>4</sub> (50 nm,

100 nm) and bulk, which probably; presents a relative good thermal stability. The weight loss of 1.93%, 2.29% and 0.84% for 50 nm, 100 nm, and bulk, respectively (*Figure 5 B-f, g, and h*), in the region of 200-400 °C, may be attributed to the release of crystal water. On the other hand, the TGA curve of the small size (6 nm) was very complex as shown in the *Figure 5*. The weight loss in the temperature range of 26-100 °C is about 4.85% corresponding to the release of physically absorbed water and the residual solvent in the sample. In the temperature range 100-450 °C there still exists a gradual weight loss of 5% which is due to the organic surface modification. There was another stage of weight loss of 1.2% observed in the temperature range of 730-830 °C, which may be due to the deoxidation of FeO. The total weight loss from the graph of synthesized nanoparticles (*Figure 5*) was 11.33%, 5.31% and 6.2%, respectively for 6 nm, 50 nm, and 100 nm indicating the transition phase from Fe<sub>3</sub>O<sub>4</sub> to FeO. The experiment result shows the toxicity effects of the different sizes of nano-Fe<sub>3</sub>O<sub>4</sub> particles and bulk-Fe<sub>3</sub>O<sub>4</sub> might depend on the chemical composition, the structure properties/ particle sizes, the concentration in the tested medium, the time of incubation, as well as the plant species.

The phytotoxicity effects of Fe<sub>3</sub>O<sub>4</sub> NPs (6 nm, 50 nm, 100 nm ), and bulk were evaluated in cucumber (*Cucumis sativus* L ) plants grown in hydroponic conditions in terms of growth parameters, biomass production, TEM observation, antioxidant enzyme activities and MDA content. The results show that among the synthesized nano-Fe<sub>3</sub>O<sub>4</sub> (6 nm, 50 nm and 100 nm ), only the small size (6 nm ) was observed to have significant inhibition on fresh and dry biomass of cucumber plants. Nano-and bulk-Fe<sub>3</sub>O<sub>4</sub> treatments (21days) caused more oxidative stress in cucumber plants. Cucumber plants grown under lowest concentrations of 50 mg/L nano-Fe<sub>3</sub>O<sub>4</sub> (6 nm) were affected by a decrease in biomass and enzyme activities compared to the control. However, at higher concentration of nano-Fe<sub>3</sub>O<sub>4</sub> dosage (2000 mg/L), there was significant increase in biomass and enzymatic activities (SOD and POD) respectively. The phytotoxicity effects of the different sizes of nano-Fe<sub>3</sub>O<sub>4</sub> particles and bulk-Fe<sub>3</sub>O<sub>4</sub> might depend on the chemical composition, the structure properties/particle sizes, the concentration in the tested medium, the time of incubation, as well as the plant species.

## Conclusion

The results showed that, nano-Fe<sub>3</sub>O<sub>4</sub> (2000 mg/L) did not change the toxicity of the tested heavy metals at high concentration (10 mM) in the seedlings of cucumber. Addition of magnetic (Fe<sub>3</sub>O<sub>4</sub>) nanoparticles (2000 mg/L) in each metal solution (1 mM), significantly decreased the growth inhibition and activated protective mechanisms to alleviate oxidative stress induced by heavy metals in the cucumber seedlings. The reducing effects of nano-Fe<sub>3</sub>O<sub>4</sub> against heavy metals stress could be dependent on the increase in the enzyme activity (SOD and POD), but also their adsorption capacity of heavy metals.

**Acknowledgements.** This work was supported by the National Natural Science Foundation of China (No. 31271627) and Henan Provincial Research Foundation for Science and Technological Breakthroughs, China (Grant No. 152102110106).

## REFERENCES

- [1] Burman, U., Garg, B. K., Kathju, S. (2004): Interactive effects of thiourea and phosphorus. – *Biol. Plant.* 48: 61-65.
- [2] Garg, B. K., Burman, U., Kathju, S. (2006): Influence of thiourea on photosynthesis, nitrogen metabolism and yield of clusterbean (*Cyamopsis tetragonoloba* (L.) Taub.) under rainfed conditions of Indian arid zone. – *Plant Growth Regul.* 48: 237-245.
- [3] Jain, T. K., Richey, J., Strand, M., Lesliepelecky, D. L., Flask, C., Labhasetwar, V. (2008): Magnetic nanoparticles with dual functional properties: drug delivery and magnetic resonance imaging. – *Biomaterials* 29(29): 4012-4021.
- [4] Laurent, S., Forge, D., Port, M., Roch, A., Robic, C., Elst, L. V., Muller, R. N. (2008): Magnetic iron oxide nanoparticles: synthesis, stabilization, vectorization, physicochemical characterizations, and biological applications. – *Chem. Rev.* 39(35): 2064.
- [5] Liu, J., Sun, Z., Deng, Y., Zou, Y., Li, C., Guo, X., Xiong, L., Gao, Y., Li, F., Zhao, D. (2009): Highly water-dispersible biocompatible magnetite particles with low cytotoxicity stabilized by citrate groups. – *Angew. Chem.* 48(32): 5875.
- [6] Miguelsancho, N., Bomatímiguel, O., Colom, G., Salvador, J. P., Marco, M. P., Santamaría, J. (2011): Development of stable, water-dispersible, and biofunctionalizable superparamagnetic iron oxide nanoparticles. – *Chem. Mater.* 23(11): 2795-2802.
- [7] Roca, A. G., Marco, J. F., Morales, M. D. P., Serna, C. J. (2007): Effect of nature and particle size on properties of uniform magnetite and maghemite nanoparticles. – *J. Phys. Chem. C* 111(50): 18577-18584.
- [8] Shen, L. H., Bao, J. F., Wang, D., Wang, Y. X., Chen, Z. W., Ren, L., Zhou, X., Ke, X. B., Chen, M., Yang, A. Q. (2013): One-step synthesis of monodisperse, water-soluble ultra-small Fe<sub>3</sub>O<sub>4</sub> nanoparticles for potential bio-application. – *Nanoscale* 5(5): 2133.
- [9] Vinod, K., Awasthi, G., Chauchan, P. K. (2012): Cu and zn tolerance and responses of the biochemical and physiochemical system of cucumber. – *J. Stress Physiol. Bi.* 8(3).
- [10] Xiao, L., Li, J., Brougham, D. F., Fox, E. K., Feliu, N., Bushmelev, A., Schmidt, A., Mertens, N., Kiessling, F., Valldor, M., Fadeel, B., Mathur, S. (2011): Water-soluble superparamagnetic magnetite nanoparticles with biocompatible coating for enhanced magnetic resonance imaging. – *Acs Nano* 5(8): 6315.